BIFROST: High-Performance Multipath Reliable Transport in Alibaba VPC Network

Paper #64, 12 pages body, submitted to Operational Systems Track

Abstract

Virtual private cloud is the foundation of multi-tenant networking in Alibaba Cloud, carrying the traffic of diverse tenant services. Over 80% of these services depend on reliable transport to ensure correctness and performance. However, today's VPC still relies on unreliable overlays such as VXLAN and delegates reliability to guest TCP stacks, which struggle under large-scale deployments with inevitable network instabilities.

In this paper, we present BIFROST, a high-performance multipath reliable transport framework for VPC networks. BIFROST operates entirely within the virtualization stack, remaining transparent to both tenants and underlay infrastructure. It ensures in-order delivery via in-place guest reordering, achieves end-to-end reliability with delayed bitmap ACKs, and employs efficient reliability state management to support large-scale deployment. Extensive evaluation shows that BIFROST reduces tail latency by up to 307× for Redis and 66× for Nginx, improves failure recovery, and supports O(1M) concurrent connections per SmartNIC.

1 Introduction

Virtual Private Cloud (VPC) provides cloud tenants with a fundamental overlay network that enables isolated, self-managed networking environments. It has become an increasingly important infrastructure-level service for major cloud service providers (CSP) [11,16,32,45]. In Alibaba Cloud, the number of VPC has more than doubled from 3.2 trillion to 8.0 trillion over the past five years. Our statistics reveals that of all tenant application services over 80% depend on reliable transport (RT), and more than 50% are sensitive to tail latency [28]. Current VPC implementations rely on guest-side TCP for RT. However, our observation shows that TCP suffers significant performance degradation in the presence of network instabilities such as NIC flapping, elephant flows, and losses on virtual NICs (vNICs), which are not uncommon in production clouds. This is mainly because TCP uses single-path transmission and coarse-grained retransmission timeout (RTO).

Recent work has explored multipath transmission to improve the performance of RT. One line of work accomplishes this by customizing functions in programmable switches [1, 13, 31, 35–37, 56, 63, 65, 71, 72, 76]. Another line of work modifies the network stack, either on the guest side [22,29,52,61,80] or the host side [19,21,30,36,38,41,44,57,58,62,67,78,79]. Only a limited number of these studies explicitly address network virtualization and they invariably adopt the host-side approach [19,44,57,58,67]. In Alibaba Cloud, we implement multipath RT on the host side, because not all switches in the cloud are programmable, and modifying guest-side network stack is intrusive for tenants. More specifically, our implementation is constrained to VPC's network virtualization layer, which serves as the interface between the virtual overlay network and underlying physical fabric. This strategic positioning has the additional advantage of facilitating loss detection across the entire datapath to enforce end-to-end reliability guarantees.

Implementing high-performance multipath RT in the host-side virtualization stack remains challenging, as evidenced by our experience of operating large-scale VPCs [39,40,73]:

- **Handling out-of-order packets.** Elephant flow mitigation typically requires packet spraying, which generates significant out-of-order (OOO) packet delivery at the host. Direct delivery of such OOO packets to the guest would trigger spurious retransmissions and significantly degrade the performance. In contrast, ensuring in-order delivery requires substantial buffering [62], typically in SRAM for the sake of throughput. Under a common production condition of 200Gbps bandwidth and 1ms RTT, this will require 25MB of memory. However, the virtualization stack is increasingly offloaded to SmartNICs, which provide only O(10MB) of SRAM to be shared by multiple packet-processing functions. The reorder buffer would create a substantial memory pressure, making in-order delivery challenging.
- **Reliable coverage.** In VPC networks, packet losses can occur in both physical links and virtualized in-host paths, especially on vNICs. A naive approach is to let the tenant vNIC notify BIFROST upon packet receipt, but this requires tenant stack modification and is therefore intrusive. The challenge remains to achieve reliability that covers the en-

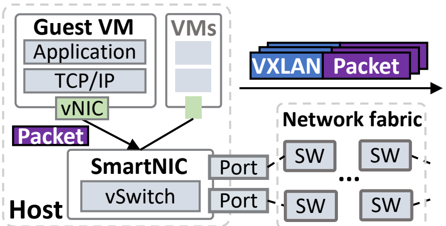

Figure 1: The basic architecture of VPC.

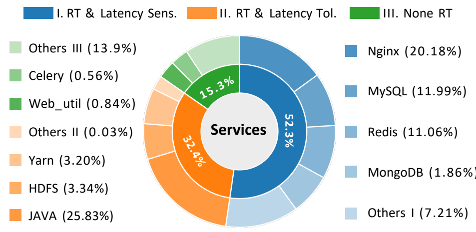

Figure 2: Service distribution.

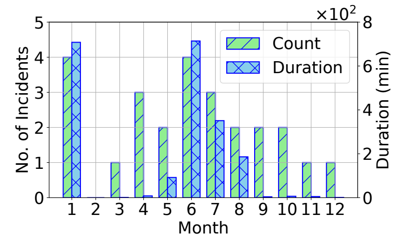

Figure 3: Failures in RT services.

tire datapath while staying transparent to tenants.

- **Scalability.** In our production environment, a single SmartNIC in the largest VPC already sustains up to $O(1\text{M})$ concurrent connections, making it challenging to maintain reliability states under the limited resources of SmartNICs.

To address these challenges, we propose BIFROST, a high-performance multipath RT framework for VPC networks. BIFROST introduces RTT-aware multipath packet spraying to mitigate network instabilities (§4.1); achieves near-zero-buffer in-order delivery via in-place guest reordering, where the SmartNIC places OOO packets directly into guest memory and reorders only packet metadata (§4.2); ensures end-to-end reliability and fast loss recovery through bitmap-based delayed ACKs (§4.3); and scales to $O(1\text{M})$ connections by combining connection aggregation, sender-side delayed release, and resource pooling (§4.4). We have been developing BIFROST for a year with internal deployments in Alibaba Cloud (§5). Our evaluation shows that BIFROST reduces tail latency and sustains high throughput for critical services under various network conditions (§6). The insights and lessons from BIFROST can offer valuable guidance for the academic community and other cloud vendors (§7).

Our major contributions are as follows:

- We present extensive operational data and cases from Alibaba Cloud, which reveal reliability challenges in VPC and motivate our design of multipath reliable transport.
- We propose BIFROST, a high-performance multipath RT framework, which combines RTT-aware multipath packet spraying with in-place guest reordering, bitmap-based delayed ACK, and efficient reliability state management.
- For deployment in VPC, we implement BIFROST with several techniques. BIFROST integrates with the vSwitch architecture, decouples control and data paths for SmartNIC offload, preserves core affinity via flow redirect, and enables protocol version negotiation to ensure compatibility.
- BIFROST has undergone a year of development and internal deployment in Alibaba Cloud. BIFROST improves RT service performance, reducing tail latency by up to 307× for Redis and 66× for Nginx. BIFROST reduces memory consumption by 64.7%, thereby supporting $O(1\text{M})$ connections per SmartNIC. We also share our lessons and insights.

2 Background and Motivation

In this section, we present the VPC architecture and describe the current state of RT services in the cloud (§2.1). We further discuss the network instabilities (§2.2), based on our monitoring data from large-scale deployment and operations.

2.1 VPC Architecture and RT Service

VPC architecture. VPC provides the foundation for tenant isolation in modern cloud infrastructure, organized in a hierarchy across the VM, SmartNIC, and switching fabric (Figure 1). Inside each VM, the guest OS runs a full network stack (*e.g.,* TCP/IP) and interfaces with a vNIC exposed by the host to exchange data. The host, *i.e.,* the physical server, is equipped with a SmartNIC—CIPU [25], an in-house SmartNIC developed by Alibaba Cloud. The CIPU executes core network virtualization logic and hosts the Apsara vSwitch (AVS) [39], which serves both as the endpoint of the physical network and the tunnel ingress for virtualized tenant networks. AVS supports tenant functions such as isolation [11], ACLs [5], and routing [6], and also handles VXLAN encapsulation for tenant traffic. It also provides observability tools such as Traffic Mirroring and Flowlog [3, 4, 14, 15], and adopts a hybrid hardware–software design for high throughput, programmable control, and hot upgrades [73].

RT services landscape. We present the distribution of services across all applications across Alibaba Cloud [28]. We classify these services into two main categories: RT and non-RT. The RT services are further subdivided based on their sensitivity to tail latency. Tail-latency-sensitive services are highly sensitive to even a small percentage of high-latency packets, while tail-latency-tolerant services can endure a certain degree of slow packets without a severe performance impact. As shown in Figure 2, RT applications dominate the service landscape, accounting for 84.72% of all services. Among these services, more than 60% are tail-latency-sensitive, including critical applications such as Redis [54], Nginx [68], MySQL [49], and MongoDB [46]. Currently, these applications rely on guest-OS transport protocols such as TCP for RT. However, due to inherent limitations, such as single-path transmission and coarse RTO, TCP is unable to handle network failures. Our year-long incident analysis of RT services (Figure 3) shows peak months with up to four failure incidents, accumulating over 700 minutes of service disruption and causing substantial customer impact. Given the critical role of RT services, it is imperative to provide these services with high-performance RT capabilities within the VPC.

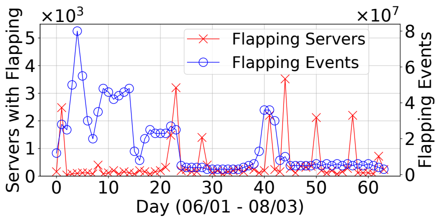

Figure 4: Daily physical NIC flapping.

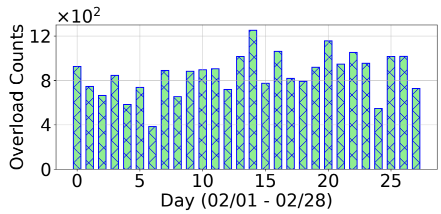

Figure 5: Daily AVS CPU overload.

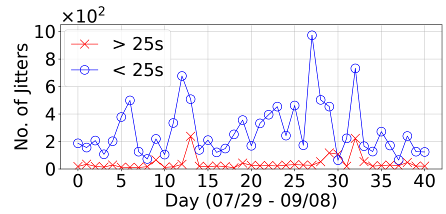

Figure 6: Daily physical network jitter.

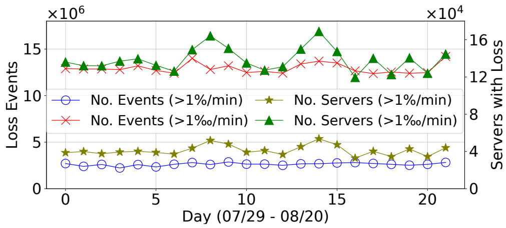

Figure 7: Daily packet loss in physical NICs.

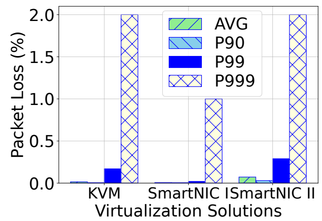

Figure 8: Packet loss in vNIC.

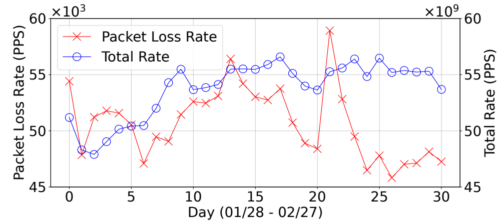

Figure 9: Daily packet loss in CGW.

2.2 Network Instabilities in Large-Scale Cloud

Based on our experience, we observe that service disruptions typically stem from instabilities in large-scale network infrastructure. We present statistical results from our monitoring below, with representative operational cases in Appendix B.

Host-side instabilities. In the production environment, a substantial fraction of reliability incidents originate within the physical host, where packets traverse multiple in-host segments, from physical NICs to the AVS, before reaching the tenant VM. Such instabilities can be categorized as follows.

Physical interface instability. NIC flapping (Figure 4) occurs when physical interfaces intermittently change link states, causing transient packet loss. From our two months of production monitoring across the entire cloud [1], we observe daily peaks of thousands of affected servers and millions of flap events. Such disruptions force applications to re-establish connections, adding latency and risking SLA violations. Beyond flapping, other factors such as bursty congestion also contribute to packet loss. To quantify their impact, we collect per-minute packet loss data from all physical NICs over a 20-day period (Figure 7). We define a loss event as any one-minute interval during which the packet loss rate exceeds 1%. Under this definition, O(10k) servers experience O(1M) loss events daily; at a 1‰ threshold, this expands to O(100k) servers with O(10M) events per day. These pervasive losses inflate tail latency and trigger retransmissions, driving SLA violations in latency-sensitive services.

In-host path congestion. Within the host, we also observe frequent CPU overload in the AVS datapath (Figure 5). From one-month monitoring in a production region [2], *hundreds* of overload events are recorded daily, defined as the utilization per core that exceeds 80%. Such sustained overload directly impacts packet processing latency and leads to *vNIC packet loss*. In virtualized environments, vNIC packet loss occurs when receive queues overflow because the host-side AVS is overloaded or the guest CPU drains packets too slowly. we monitor a typical production region and analyze the loss across different virtualization solutions. As shown in Figure 8, the P999 loss rate across all servers in this region exceeds 1% over a 12-hour period for all solutions evaluated, making it an important source of reliability incidents.

[1]The entire cloud contains O(1M) servers.

[2]This region contains O(100k) servers.

> ***Takeaway 1:*** *Host-side instabilities motivate* ***(i) multipath transmission*** *to bypass flapping interfaces and* ***(ii) reliability coverage*** *across virtualized in-host paths.*

Network-side instabilities. The physical network datapath also experiences persistent, though less frequent, instabilities that nonetheless cause noticeable disruptions.

Elephant flows. In practice, a small fraction of long-lived, high-volume flows can dominate link and CPU resources. Under TCP's single-path constraint, such flows are pinned to a single path, overloading the corresponding host-side CPU core. Hash collisions can then place multiple elephant flows onto the same path, further aggravating congestion. According to prior analysis [42, 50, 66, 74], elephant flows contribute to 7.8% of such overload events in Figure 5. These hotspots not only degrade the flow itself but also impair co-located traffic.

Network jitter. In production networks, jitter—caused by transient congestion, dynamic switch buffers, and hardware pipeline delays—remains a persistent instability. As shown in Figure 6, 40 days of telemetry from one region reveal *hundreds* of sub-25s and *dozens* of >25s jitter bursts per day, indicating that jitter is a recurring phenomenon rather than a rare anomaly. Such jitter disrupts pacing, inflates queues, and triggers timeouts in latency-sensitive applications.

> ***Takeaway 2:*** *Network-side instabilities necessitate* ***(i) packet spraying*** *to disperse elephant flows and* ***(ii) path-quality awareness*** *to avoid degraded paths under jitter.*

Middlebox instabilities. In scenarios such as Cloud Enterprise Network (CEN) deployments or general inter-region connectivity [7], traffic often traverses multiple CPU-based middleboxes—Gateways (GW), Load Balancers (LB), and Transit Routers (TR) [8–10]—whose limited capacity makes them prone to overload. When per-flow cores saturate, bottlenecks cause buffer overflows and packet drops. As shown in Figure 9, our month-long monitoring of unplanned packet loss in Cloud Gateway (CGW) shows that, although the average loss rate is below 0.01%, the massive traffic volume in CSP networks still results in $O(10\text{k})$ dropped packets per second.

Takeaway 3: *Packet losses from middlebox and host-side instabilities, coupled with TCP's coarse RTO, inflate tail latency and motivate* ***fast loss detection and recovery****.*

2.3 Potential Solutions and Their Issues

While numerous efforts have been made to address the above issues [1, 13, 19, 21, 22, 29–31, 35–38, 41, 44, 52, 56–58, 61–63, 65, 67, 71, 72, 76, 78–80], existing solutions still face various issues that limit their practical adoption in VPC. We categorize the limitations into three key issues:

Limited performance improvement. Flow- or flowlet-level multipath solutions [36, 37, 52, 71, 72] often struggle under elephant flows due to their coarse granularity. PLB [52] and LetFlow [71] rely on random repath reselection, slowing convergence. MPTCP [29, 61] incurs Head-of-Line (HoL) blocking during reordering and shows limited benefits in cloud settings [23]. SRD, Strack, REPS [21, 38, 57, 58] adopt packet spraying but lacks reordering support at the receiver, incurring spurious retransmissions from OOO arrivals.

Intrusiveness to users. *Guest-side* solutions [22, 29, 52, 61, 80] like MPTCP and PLB require guest stack modifications, making them intrusive to deploy. Solutions like Clove, PLB and Flowbender [35, 36, 52] rely on ECN, which is typically disabled on end hosts [66], requiring user intervention.

Poor compatibility and scalability. *Switch-side* solutions [1, 13, 31, 35–37, 56, 63, 65, 71, 72, 76] rely on customized switch functions for adaptive routing or in-network reordering, which are not universally available in large-scale networks. Based on our operational experience, physical switches are not well-suited to upgrade frequently due to their large failure radius. Our online failure recovery service ZooRoute [67] shows that 36.12% of intra-region link failures (2025/05/01–2025/09/01) stem from switch anomalies. In addition, some approaches [1, 20, 26, 51] depend on central servers, limiting their scalability for large-scale deployments.

2.4 Design Rationale and Challenges

Design goals. Building on the takeaways from §2.2 and the deficiencies identified in §2.3, achieving high-performance multipath RT requires three key objectives:

Link-aware packet spraying. Traffic must be sprayed across multiple paths based on real-time path quality to escape failures, bypass congestion, and disperse elephant flow hotspots.

Receiver-side in-order delivery. Packet spraying inevitably causes OOO arrivals; reordering must be completed before the guest stack to avoid spurious retransmissions.

End-to-end loss detection and fast recovery. Packet losses must be accurately detected across both physical and virtualized segments of the entire VPC datapath and promptly recovered to minimize disruption.

Design choice. To realize these goals, the first question is where in the network stack to implement high-performance multipath RT. Existing designs span three positions: (i) *switch-based* customization, (ii) *guest-based* modification, and (iii) *host-based* enhancement. *Guest-based* designs are intrusive to tenants, while *switch-based* designs require hardware upgrades with poor compatibility and scalability. We therefore place our design in the host-side virtualization stack, which serves as both the endpoint of the physical network and the ingress of the virtual overlay. This dual role makes it a natural layer for end-to-end reliability and cloud-wide deployability without tenant or physical switch changes.

Challenges. Realizing these goals on the host-side stack is non-trivial: the complex virtualized datapath and the limited resources of CIPUs raise three fundamental challenges.

Handling OOO packets. Packet spraying improves robustness but induces OOO arrivals, which naively demand NIC hardware SRAM buffering [62]. The challenge is to reorder efficiently within the scarce hardware SRAM of CIPU.

Reliability across the full VPC datapath. The challenge is to extend reliability beyond physical links to cover virtualized in-host paths (*e.g.,* vNICs), while staying transparent to tenants.

Scaling reliability with limited CIPU memory. Maintaining reliability state for $O(1\text{M})$ connections in production stresses limited CIPU memory [3], which requires carefully balancing between reliability and resource efficiency for scalability.

3 Design Overview

In this section, we present the design of BIFROST. We begin with an overview of BIFROST (§3.1), followed by a brief description of its protocol design (§3.2).

3.1 BIFROST Overview

Figure 10 illustrates the system overview of BIFROST, which integrates several key components for high-performance multipath RT in VPC, including RTT-aware multipath packet spraying, in-place guest reordering, loss detection via a delayed ACK bitmap and efficient reliability state management. The four optimizations aim to address the challenges analyzed in §2.4. The main workflow of BIFROST is as follows.

When a VM sends a packet, it remains buffered in guest memory until acknowledged. The reliable transport engine

[3] In practice, even our most capable CIPUs have only 64 GB DDR memory shared by compute, storage, and networking hypervisors. Measurements across $O(10\text{k})$ servers show some NIC memory nearing saturation, with utilization at 34% (P99), 93% (P999), and 96% (P9999).

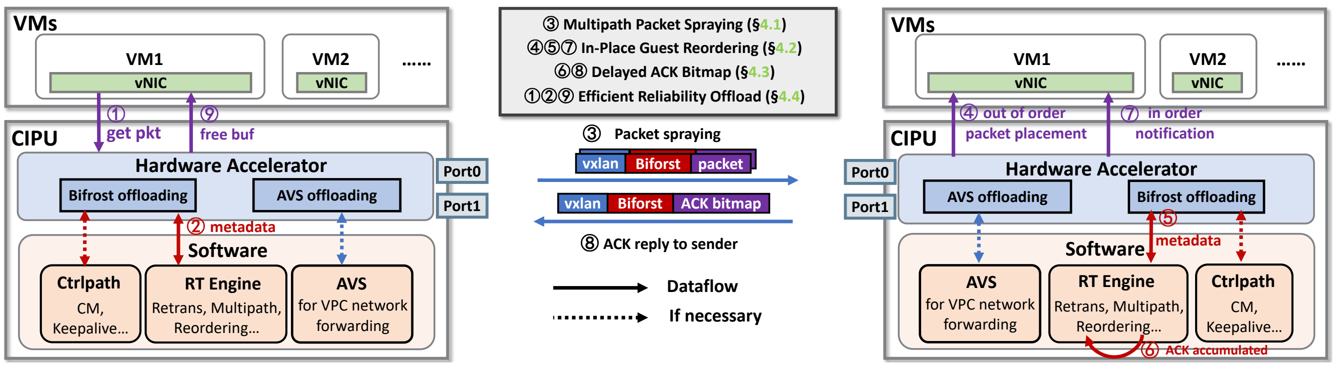

Figure 10: BIFROST overview.

(RTE) and AVS process the packet and spray it across multiple physical paths based on historical RTT measurements (§4.1). On the receiver side, OOO packets are placed directly into the guest memory of the destination VM without extra buffering on the CIPU. The RTE then reorders the associated packet metadata and issues an in-order notification to the VM (§4.2). Once a packet is transferred into guest memory, it is considered delivered. The RTE generates ACKs, which are aggregated into a bitmap and sent to the sender (§4.3). Upon receiving the ACK bitmap, the sender performs loss analysis, identifies missing packets for retransmission, and releases the corresponding buffers for acknowledged packets (§4.4).

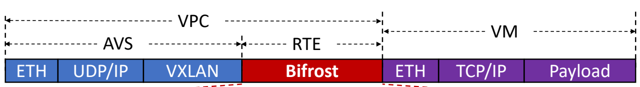

Bits 0-7	8-11	12-15	16	17	18	19	20	21-23	24-31
Pkt Type	Version	CC Type	se	ack	dir	ece	ret	Path ID	Reserved
Packet Sequence Number (PSN)									
Destination Connection ID (CID)									
Timestamp Value									

Figure 11: Bifrost protocol format.

3.2 BIFROST Protocol

Figure 11 illustrates the protocol stack of BIFROST. Positioned above the VXLAN layer but beneath the tenant packet, BIFROST introduces a lightweight header that extends the virtualization boundary embedding RT semantics while remaining fully transparent to guest applications. The figure also shows the format of a data packet header. Several fields are particularly important for subsequent mechanisms: *Version* enables protocol version negotiation across heterogeneous NICs; the *Path ID* identifies paths within a multipath connection and enables packet-level steering; the *Packet Sequence Number* (PSN) provides fine-grained support for reordering at the receiver side; the *Connection ID* (CID) identifies a connection and is exchanged during connection establishment; and the *Timestamp Value* field enables precise RTT measurement for path quality estimation. These fields form the foundation of our design and deployment, with detailed specifications provided in Appendix C.

4 BIFROST Design

4.1 RTT-Aware Multipath Packet Spraying

To handle failure escape and elephant flow hotspots, BIFROST uses RTT-aware multipath packet spraying: packet-level spraying disperses elephant flows and avoids hash collisions, while RTT-guided selection steers traffic to healthy paths.

Packet spraying strategy. BIFROST maintains an RTT table that records the latency and availability of each candidate path. Each flow is divided into small packet groups (*e.g.,* 50 packets per group), and BIFROST selects the *top-k* (*e.g.,* 4) paths with the lowest RTTs for transmission. These packet groups are then distributed across the selected paths in a round-robin fashion. For deterministic path selection, each physical path is mapped to a distinct *srcPort* in the outer five-tuple, and BIFROST rewrites this field to select the intended path.

RTT measurement. Accurate RTT tracking is critical for responsive path quality detection. For active paths, BIFROST piggybacks RTT measurement on data traffic by extracting *Timestamps* from ACK packets and updating the RTT table via exponential smoothing. This prevents transient spikes from causing unnecessary path switching, while still allowing the system to converge quickly when path quality genuinely changes. For idle paths that have seen no traffic for extended periods, the control plane periodically sends lightweight probes to maintain keepalive and refresh RTT. This dual strategy keeps BIFROST 's path-quality view fresh on both active and idle paths, enabling fast failure detection and rerouting.

4.2 In-Place Guest Reordering

To handle reordering from multipath spraying, we design an in-place guest reordering (IPGR) mechanism at the receiver (Figure 12). A naive approach buffers all OOO packets on the SmartNIC hardware SRAM until the missing ones arrive [62], which requires reorder buffers and quickly exhausts the limited on-card resources. Our key insight builds on the de facto paravirtualized I/O interface (*virtio*) [55], which is ubiquitously deployed in large-scale clouds. In *virtio*, the VM consumes packets not in the order they are written into memory, but in the order their *descriptors* are written into the *used*

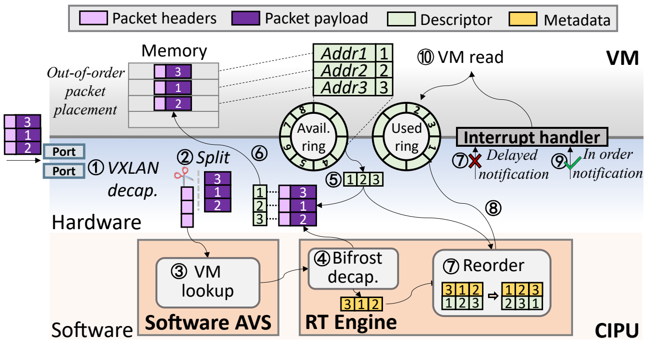

Figure 12: The workflow of in-place guest reordering.

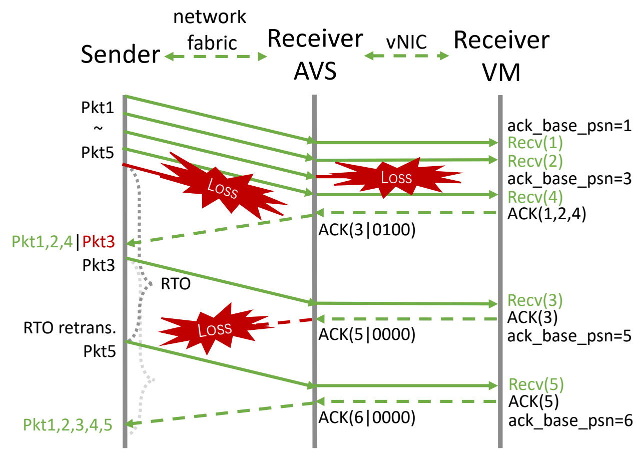

Figure 13: Loss detection via delayed ACK bitmap.

ring. Leveraging *virtio's two-level mapping*, IPGR enables in-order delivery with near-zero buffering on the CIPU.

Out-of-order packet placement. Upon packet arrival, the CIPU hardware decapsulates the VXLAN header (①) and separates headers from payload for further processing (②). The headers are passed to the AVS to identify the destination VM (③) and then to the RTE for Bifrost header decapsulation (④). Instead of buffering the OOO packets on the CIPU, the hardware fetches a descriptor from the VM's *available ring* (⑤) and DMA-transfers those packets into guest memory (⑥). As a result, packets are placed in guest memory in the exact order they arrive, while only their metadata (PSN and descriptor) is retained for subsequent reordering.

In-order notification to guest. To reconstruct in-order delivery, Bifrost RTE reorders only the metadata associated with each packet. After sorting, the hardware writes the sorted *descriptors* into the *used ring* in the correct sequence and notifies the VM to consume the packets. From the guest's perspective, packets are consumed strictly in order from the *used ring*, even though they are placed in memory out of order. As illustrated in Figure 12, steps ⑤⑥⑦⑧ show this process: although packets are DMA-placed into guest memory in the arrival order $3 \rightarrow 1 \rightarrow 2$ (*addr*[1]=3, *addr*[2]=1, *addr*[3]=2), the RTE reorders their metadata and writes the indices to the *used ring* in the sequence *addr*[2], *addr*[3], *addr*[1].

Delayed interrupt for in-order notification. To ensure that the guest never observes OOO packets, Bifrost introduces a *delayed interrupt notification* mechanism. In the default *virtio* design, an interrupt is raised immediately after a packet is delivered into guest memory (*i.e.,* right after step ⑦ in Figure 12), which risks exposing OOO packets to the VM. To avoid this, Bifrost defers the interrupt until step ⑨, after reordered *descriptors* have been written into the *used ring*. This ensures the VM is interrupted only when in-order packets are ready for consumption.

Overall, IPGR achieves in-order delivery with near-zero overhead. Only metadata is buffered on the CIPU, while packets are transferred into guest memory immediately using the standard virtio buffers, incurring no extra memory burden to the VM. The temporary footprint on guest memory is negligible (KBs vs. the tens of GBs typically provisioned for VMs). The performance impact is also minimal, since only headers and metadata are exchanged between hardware and software during reordering, rather than full packets. Finally, IPGR is implemented entirely on the CIPU side, requiring no guest changes and remaining transparent to tenants.

4.3 Loss Detection via Delayed ACK Bitmap

To enhance reliability and achieve fast loss recovery, we redesign the ACK and loss recovery mechanism.

ACK aggregation via delayed bitmap. We redesign the ACK mechanism with two techniques for accurate and efficient delivery confirmation. First, to extend reliability coverage across the entire VPC datapath, including virtualized segments (*e.g.,* vNICs), we introduce the *delayed ACK*. Unlike naive design that acknowledges a packet once it reaches the host, Bifrost defers ACK generation until the packet has been delivered into the guest memory by the AVS. This ensures that every ACK strictly reflects packets visible to the guest. Second, to efficiently track the delivery status of multiple packets, we employ a *bitmap-based selective ACK*, which encodes the receipt status of a sequence of packets into a compact bitmap. The sender can thus quickly infer both received and missing packets from the bitmap.

Fast loss detection and recovery. To achieve fast loss recovery, Bifrost combines bitmap-based gap detection with microsecond-scale retransmission timeout (RTO). Upon receiving an ACK bitmap, the sender detects discontinuities in the PSN sequence and immediately triggers fast retransmission. For tail losses, where no discontinuity appears in the bitmap, and for cases where ACKs are lost, Bifrost relies on an microsecond-precision RTO fallback. The initial RTO starts at 4 ms (roughly 2 RTTs) and grows exponentially for subsequent retransmission of the same packet (*e.g.,* 8 ms, 16 ms, ...), ensuring timely loss recovery.

We illustrate this process in Figure 13. When the sender transmits packets `1-5` and the receiver VM receives only `1, 2, 4`, the AVS generates an `ACK(3|0100)`. This bitmap means that all packets with PSNs less than `3` have been received. Starting from PSN `3`, the bitmap `0100` indicates that the packet with PSN `4` is received, but packets with PSN `3` is lost. BIFROST triggers fast retransmission of packet `3`. When the receiver VM later receives packet `3`, all packets with PSNs below `5` have been received, and the AVS generates `ACK(5|0000)` to return to the sender. However, this ACK is lost during transmission. At the same time, packet `5` times out on the sender due to RTO and is retransmitted. When the VM receives the retransmitted packet `5`, the AVS generates `ACK(6|0000)` and sends it to the sender. After receiving the ACK, the sender confirms that packets `1-5` have been successfully delivered, thus finalizing transmission.

4.4 Efficient Reliability State Management

RT requires maintaining both per-connection state and packet caches for potential retransmissions. At cloud scale, with millions of tenants and highly concurrent connections, these overheads put heavy pressure on CIPU memory and limit scalability. To mitigate this, BIFROST applies a set of resource allocation optimizations that reduce memory overhead.

Connection aggregation. Within a VM, a transport connection is fundamentally established at the 5-tuple granularity, uniquely identified by the combination of *protocol*, *IPs*, and *ports*. A straightforward mapping of every 5-tuple onto a dedicated BIFROST connection on the CIPU would result in a large number of active connections, quickly exhausting limited SmartNIC memory and undermining scalability. To address this, BIFROST introduces a vNIC-level aggregation mechanism: instead of maintaining per-5-tuple state, all flows between the same pair of source and destination vNICs are multiplexed onto a single logical BIFROST connection. However, such aggregation inevitably introduces potential HoL blocking across multiplexed flows, and the trade-off between aggregation granularity and HoL risk is discussed in §7.3. Through careful balancing, the vNIC-pair granularity achieves substantial scalability gains while confining HoL impact within well-defined boundaries.

Sender-side delayed release. To ensure reliable transport, the sender must temporarily retain unacknowledged packets to enable potential retransmissions. A naive design would buffer the full payloads on the CIPU until corresponding ACKs arrive. However, since the tenant VM's TCP stack already keeps a copy of each outstanding packet, duplicating the same data on the CIPU not only wastes memory but also severely limits scalability in large-scale clouds. To eliminate this redundancy, BIFROST adopts a sender-side delayed release mechanism: the CIPU stores only lightweight metadata, including the packet descriptor, instead of full packets, while the actual packets remain pinned in the VM. If retransmission is needed, the CIPU uses the *descriptor* to fetch the packet from VM memory and resend it. Once the ACK is received, the CIPU releases the *descriptor* to the *used ring*, allowing the VM to reclaim the buffer. Note that this mechanism requires support from programmable NIC hardware, as the default workflow would immediately recycle *descriptors* after transmission. The detailed default and optimized workflows are illustrated in Appendix D.

Resource pooling. Reliable transport requires maintaining per-connection state. A naive approach is to statically reserve these transmission resources for every established connection, regardless of activity. At cloud scale, this static reservation quickly exhausts CIPU memory, as many connections may remain idle at any given time. BIFROST instead adopts a demand-driven pooling mechanism that allocates resources only for *active* connections. Connection-related structures, such as queues and TX/RX windows, are backed by a global pool. The per-packet resources within these structures (*e.g.,* metadata entries) are dynamically allocated on demand upon packet arrival, while idle connections consume only minimal memory. For example, the naive design reserves 256 metadata entries (16 bytes each) per connection, with these entries consuming over 40% of the TX window footprint. BIFROST replaces this with dynamic allocation from a shared metadata pool, provisioning entries only when needed.

5 BIFROST Implementation

5.1 Deployment Issues

Several deployment issues must be addressed.

Offloading BIFROST to CIPU. The CIPU typically consists of a hardware accelerator (*e.g.,* FPGA or ASIC) for datapath processing with an embedded SoC (typically ARM cores) for control-plane software. This architecture forms the foundation of Alibaba Cloud's virtual networking stack, supporting services such as the AVS fastpath/slowpath for high-performance packet processing [39]. When offloading BIFROST to the CIPU, we face three major challenges. (1) Partitioning functionality between the hardware datapath and the SoC control plane to balance efficiency and flexibility. (2) Exploiting multi-core performance on the SoC while preserving per-connection consistency. (3) Integrating BIFROST with existing AVS logic for seamless multipath RT support.

Adaptation to heterogeneous NICs. In production-scale clouds, server fleets are highly heterogeneous: even within a single region, servers may use different generations of CIPUs or legacy commercial NICs with no programmability. To enable cloud-wide deployment, BIFROST must operate correctly across this diverse hardware landscape and gracefully adapt to varying levels of offload capability.

5.2 Offload BIFROST to CIPU

Separation of datapath and control path. In BIFROST, the datapath and control path (ctrlpath) are explicitly separated to balance performance and flexibility. The hardware accelerator of the CIPU (*e.g.,* FPGA) is dedicated to datapath operations such as I/O, DMA, and high-speed packet forwarding. All RT-related modules, including multipath scheduling, reordering, ACK processing, loss detection, and retransmission, are

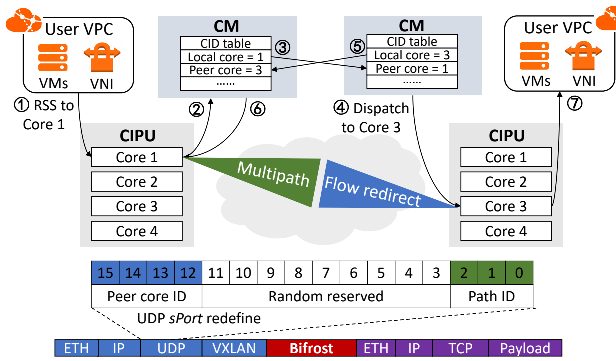

Figure 14: Workflow of flow redirect.

implemented in software on the embedded SoC cores, together with ctrlpath tasks such as connection management (CM) and keepalive. The hardware delivers only lightweight packet metadata to the RTE running on the SoC, which performs transport-level processing in software. Moreover, in architectures based on ASIC combined with a Data Process Accelerator (DPA) [48], a set of embedded RISC-V cores, the RTE modules can be directly executed on the DPA. In this case, hardware acceleration goes beyond basic I/O and DMA, allowing the entire datapath to be offloaded, while the ctrlpath remains on ARM cores for programmability.

Multi-core offload coordination. Packet processing on the CIPU naturally runs across multiple cores to scale with increasing workloads. The challenge, however, is to preserve connection consistency: *each connection must be handled by the same core at both ends for both data and ACK packets.* Any violation of this affinity breaks transport semantics and forces costly cross-core synchronization.

To address this, BIFROST establishes end-to-end core affinity at connection setup through a lightweight *flow redirect* mechanism (Figure 14). When a new connection is initiated, for example from Core 1 on CIPU 1 (①), the local CM records this core ID and triggers connection establishment (②). The sender then calls `get_sPort_for_cpuid` to compute the UDP *sPort* that the peer should use to steer return packets back to this core, and embeds this value in the connection request (③). Upon receiving the request, the remote CM extracts and stores the sender's core ID, selects a least-loaded local core to handle the connection (④), and encodes this core ID into the reply's *sPort* (⑤). Finally, the sender extracts the peer core ID from the response and stores it in the CM for future packet steering (⑥).

AVS integration and packet pipeline. The BIFROST RTE is integrated into AVS as a modular component. We next describe the BIFROST packet pipeline to illustrate how it cooperates with AVS's existing architecture.

<u>*Connection establishment.*</u> When AVS receives a packet from a local VM, it parses the packet and extracts key metadata (*e.g.*, *vPort*) to establish a vNIC-pair–level connection. Based on this information, AVS maps the packet to a CID and performs a lookup in the local CM. If no matching CID is found, BIFROST's ctrlpath initiates the connection setup procedure. The ctrlpath allocates a new CID entry and sends a connection request to the remote server. The remote server performs a similar allocation and replies with a connection response that includes its own CID and other required metadata (*e.g.*, core ID for flow redirect). After both endpoints exchange their CIDs, an RT connection is established.

<u>*Packet transmission.*</u> After connection establishment, we describe the packet processing along the TX and RX paths, where BIFROST collaborates with AVS for delivery.

TX workflow. Once a packet matches an existing CID entry in the CM, its metadata is first used by the BIFROST RTE to perform transport-level operations, including multipath selection, timer initialization, and BIFROST encapsulation. After the RTE finishes processing, the packet metadata is returned to the AVS, which then applies network functions such as ACL, routing, and VXLAN encapsulation. Then, the AVS transmits the encapsulated packet onto the physical network.

RX workflow. Upon receiving a packet, the AVS decapsulates the VXLAN header and then RTE parses the BIFROST header to determine whether it is an ACK or a data packet. If it is an ACK packet, the BIFROST RTE parses the bitmap to identify successfully delivered packets and release their corresponding resources. Any missing packets are immediately scheduled for fast retransmission. If it is a data packet, it is directly placed into guest memory. The IPGR (§4.2) guarantees in-order delivery and notifies the VM only when packets are ready in order. The BIFROST RTE then generates the corresponding ACK. Once the accumulated ACKs satisfy the bitmap threshold or no subsequent packets arrive within a timeout, an ACK bitmap is sent back to the sender.

5.3 Adaptation to Heterogeneous NICs

To achieve uniform deployment across heterogeneous hardware, BIFROST incorporates both host-based fallback and protocol-level mechanisms to ensure compatibility.

Non-programmable NICs. For non-programmable NICs, BIFROST falls back to a host-based execution path. In this setting, AVS runs on the host using DPDK [27] for packet I/O, and BIFROST integrates its reliability functions into the same pipeline. This fallback requires no additional hardware support while preserving basic correctness and end-to-end reliability, enabling uniform deployment even on legacy servers.

Protocol compatibility across heterogeneous NICs. Heterogeneous NICs offer asymmetric feature sets, which makes protocol negotiation necessary to avoid endpoint conflicts. For example, sender-side delayed release cannot be applied when reliability is offloaded to commodity DPUs (*e.g.*, NVIDIA BlueField3 [47], Intel IPU [34]), since delaying the update of the used ring requires customized hardware support. To avoid such conflicts, BIFROST introduces protocol version negotiation during connection setup: endpoints exchange their protocol *version* field in the header, and the connection is established with the maximal common feature set supported by

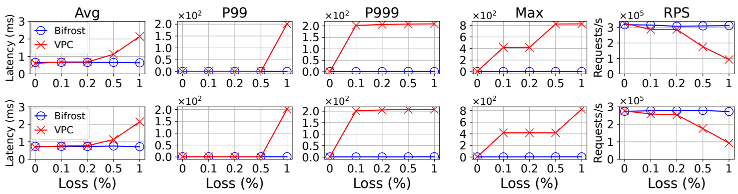

Figure 15: Redis performance (top: get, bottom: set).

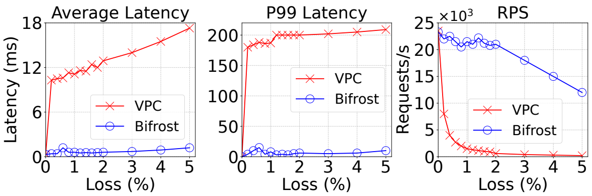

Figure 16: Nginx performance.

both versions. This ensures seamless interoperability without relying on unsupported hardware functions.

6 Evaluation

We first validate the overall performance of BIFROST (§6.1), and then use microbenchmarks to isolate and quantify the contribution of each key component (§6.2).

Experimental settings. We deploy BIFROST on Alibaba Cloud's testing clusters to evaluate its performance. These clusters closely resemble production environments and, unlike isolated lab setups, are inherently multi-tenant and may host concurrent validation or testing tasks, which exposes the evaluation to realistic interference. The clusters comprise several servers, each equipped with a CIPU powered by a CPU-FPGA architecture, whose SoC has a 16-core Intel Xeon D-1734NT CPU@2.0 GHz and 64 GB memory. The client and server VMs are placed on two different physical servers, each VM equipped with a 128-core Intel Xeon Platinum 8369B@2.90GHz and 256 GB memory.

6.1 Overall Performance

Redis. We evaluate Redis [54], a tail-latency-sensitive workload widely deployed in Alibaba Cloud. The experiments use two VMs on different physical servers, running *redis-benchmark* with persistent connections to test latency and throughput. To emulate packet loss, we configure the receiver-side AVS to drop packets at controlled rates from 0% to 1%. Figure 15 reports its latency and throughput under different loss rates. BIFROST reduces *get* latency by up to 3.4× (Avg), 242.1× (P99), 210.5× (P999), 306.9× (Max), while improving throughput by 3.4×; for *set*, the gains are up to 2.9×, 196.7×, 182.4×, 230.1×, and 2.9×, respectively. Without BIFROST, tail latency inflates sharply once loss exceeds 0.1%, with P999 and Max rising above 200 ms, leading to a collapse in throughput measured in requests per second (RPS) (from 327k to 92k at 1% loss for *get*). In contrast, BIFROST keeps tail latency below 4 ms and sustains over 300k RPS even under 1% loss of *get*. These improvements stem from bitmap loss detection and microsecond-scale RTO, enabling rapid recovery that reduces tail latency.

Nginx. We also evaluate Nginx short-connection mode under various loss rates. Its performance mirrors that of Redis. The average latency is reduced by up to 26.3×(20.2× on average), P99 latency is lowered by up to 66.7× (38.3× on average), and throughput (RPS) improves by up to 60.0× (23.9× on average). Figure 16 illustrates this stark contrast. As the loss rate climbs, the average and P99 latency in the vanilla VPC increase sharply, causing throughput to decrease to just a few hundred RPS. In contrast, with BIFROST, both average and P99 latency remain at a consistently low, under 10 ms. The throughput is also sustained, which mitigates the severe performance degradation seen in the vanilla VPC.

6.2 Per-Component Evaluation

6.2.1 Multipath Packet Spraying

We evaluate the effectiveness of BIFROST's *RTT-aware multipath packet spraying* in two representative scenarios: elephant flows and failure recovery. In both cases, we compare BIFROST against Probe-and-Switch (PS) and the vanilla VPC. PS is a path-switching approach that relies solely on probe packets to detect and migrate to alternative paths, with path probing performed at a second-level intervals to balance probing cost and responsiveness. The vanilla VPC uses default single-path transmission.

Handling elephant flows. To evaluate how BIFROST handles concurrent elephant flows, we run experiments where a client VM initiates two long-lived flows to a single server VM using *iperf*, repeating this process 100 times. On the receiver side, each NIC port is rate-limited to 3 Gbps to create a contention hotspot. For each test, we measure the bandwidth over a 5-second interval and calculate the average. We record the aggregate throughput of the two flows for each run and plot its percentile distribution for each method (Figure 17). The vanilla VPC performs poorly when two flows hash to the same receiver port due to the lack of migration, while PS mitigates this but still suffers high-percentile drops from its seconds-level convergence delay. In contrast, BIFROST maintains a consistently high aggregate throughput across all percentiles by promptly dispersing packets across multiple paths based on RTT feedback, avoiding the prolonged collisions that degrade the performance of VPC and PS.

Failure recovery. To evaluate how BIFROST responds to link failures, we use *iperf* to generate a long-lived flow from a client to a server. We record the throughput every second over a 60-second period. At the 10-second mark, we introduce artificial congestion by injecting a 10% packet loss rate on the active physical port to simulate a failure scenario, and restore the port to zero loss at the 50-second mark. As shown in Figure 18, BIFROST maintains stable bandwidth during the failure, rapidly shifting traffic away from the degraded

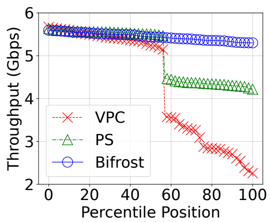

Figure 17: Flow throughput percentiles.

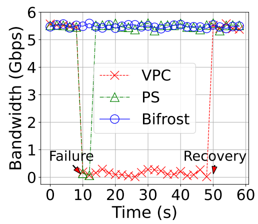

Figure 18: Impact of link failure on throughput.

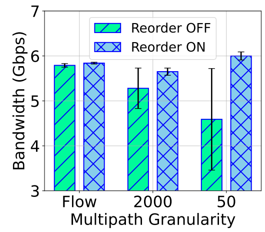

Figure 19: Bandwidth vs. granularity w/wo IPGR.

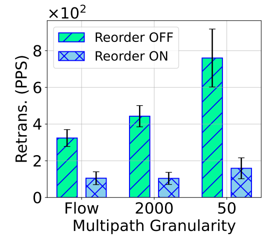

Figure 20: Retrans. vs. granularity w/wo IPGR.

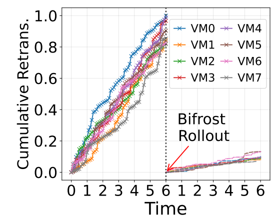

Figure 21: Cumulative retransmissions.

port to sustain performance. In comparison, VPC suffers a severe bandwidth drop and fails to recover until the port is restored, while PS achieves path switching within a few seconds but still experiences significant throughput degradation. This is because PS's second-level probing limits failure convergence time to several seconds, and VPC lacks any multipath capability to reroute around failures. In contrast, BIFROST piggybacks RTT measurements on in-flight packets, enabling rapid path quality detection and adaptive traffic redistribution.

6.2.2 Packet Reordering

We evaluate the impact of IPGR (§4.2) on performance under different multipath granularities, including flow-level, 2000-packet, and 50-packet switching. Using *iperf*, a client VM transmits a long-lived flow to a server VM under each setting. We measure bandwidth and VM's retransmissions with reordering enabled and disabled, as shown in Figures 19 and 20. Our results indicate that enabling IPGR consistently improves throughput by 1.01×–1.31× and reduces retransmission count by 3.09×–4.78× across all granularities. When reordering is disabled, finer-grained multipath results in increasingly severe throughput degradation and elevated retransmissions, as frequent path changes introduce OOO packets that trigger spurious loss recovery in the VM's transport stack. IPGR consistently achieves high bandwidth and low retransmission rates across all granularities by reordering out-of-order packets before they reach the transport stack, which shields the transport stack from spurious loss recovery, even under highly disordered packet arrivals.

6.2.3 Reliability Coverage

To verify BIFROST's reliability coverage across the full VPC datapath, we inject packet loss on the receiver side between the AVS and the vNIC, where in-host drops frequently occur. We conduct an 8-to-1 incast experiment using *iperf*, where eight client VMs on separate physical servers concurrently transmit long-lived flows to a single server VM. The injected loss rate is dynamically varied every second within a random range of 0% to 2%, and the test runs for 120 seconds. At the 60-second mark, we enable BIFROST, and we measure the cumulative retransmissions for the periods both before and after activation. As shown in Figure 21, BIFROST effectively handles in-host packet loss and prevents it from escalating to the VM, thus reducing VM retransmissions by 69.1% to 90.0%. This demonstrates that the delayed ACK mechanism ensures end-to-end reliability coverage and offloads most reliability responsibilities from the guest kernel to BIFROST.

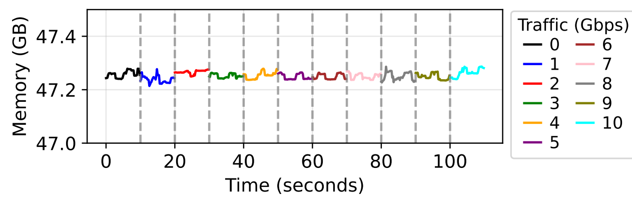

Figure 22: Memory usage on the sender-side CIPU.

6.2.4 Resources Optimization

Connection aggregation. To evaluate the benefit of connection aggregation in realistic settings, we collect connection statistics from production servers, where each server hosts multiple tenant VMs. For each server, we count the number of active connections at the 5-tuple granularity and compare it with the number of connections after vNIC-level reuse. Across hundreds of servers, connection aggregation reduces BIFROST connections by 70% on average, validating its effectiveness in production multi-tenant environments.

Sender-side delayed release. Since sender-side delayed release is hardware-dependent and not runtime-switchable, we cannot directly toggle it in experiments. To attribute its benefit, we run a single BIFROST connection between a client and a server and measure the sender's memory growth under varying traffic volumes, where the gains from connection aggregation and resource pooling are negligible. Figure 22 reports the sender-side CIPU memory usage, starting with BIFROST disabled at 0 Gbps and then enabled as traffic increases from 1 to 10 Gbps in 1 Gbps steps every 10 s. The overhead is minimal: buffering 16 bytes of metadata per packet yields only ∼500KB at 10 Gbps, orders of magnitude smaller than GB-scale full-packet caching.

Resource pooling. We evaluate how the resource pooling reduces per-connection memory overhead and improve scalability. To measure the per-connection state size, we establish a controlled number of connections from the client VM and monitor the incremental memory consumption on the sender-side CIPU. By comparing the total memory increase before and after enabling resource pooling, we compute the average state footprint per connection. Our measurements show that resource pooling reduces the per-connection state size from

34 KB to 12 KB, which improves connection scalability under the same memory budget. At this footprint, supporting 1M connections requires about 12 GB of CIPU memory, which remains within a practical range for deployment.

7 Experience

7.1 Principles of Handling Packet Loss

While our design primarily targets packet losses caused by poor link quality, we observe that in production cloud environments, a significant portion of losses stem from business-side configurations, such as access policies or bandwidth rate limiting. These losses differ fundamentally in nature and require distinct handling strategies. We therefore define two categories of loss and establish separate handling principles:

Link-quality-induced losses. These are caused by transient physical-layer impairments or congestion-related buffer drops. BIFROST fully takes over the retransmission responsibility in this case, ensuring timely and reliable recovery without relying on slow guest retransmission timers.

Policy-based drops. These are intentional drops due to business logic or security policy enforcement, and are further subdivided into two cases.

ACL and security group drops. In this case, these drops are caused by access control policies that silently discard packets at the receiver side. Since such losses are not observable by BIFROST, the receiver should not trigger retransmissions. To maintain end-to-end correctness, BIFROST synthesizes ACKs for the discarded packets, allowing the sender to progress its window as if the packets were successfully delivered.

Rate-limiting drops. When packet drops are caused by bandwidth enforcement policies, BIFROST must detect and react accordingly. Specifically, the receiver marks the dropped packets in the ACK bitmap. Upon receiving this feedback, the sender interprets the loss as a signal of rate enforcement and adaptively reduces its congestion window based on the RTT of the dropped packets, thus honoring the rate limit policy.

7.2 Applicable Workloads of BIFROST

In-memory databases (*e.g.,* Redis SET/GET). Such services are highly sensitive to tail latency and minor packet loss, where BIFROST's fast loss recovery improves P99.9 response times—crucial for latency-critical applications such as financial trading and online gaming.

Global acceleration (GA) services. GA traffic traverses long-haul cross-region links where minute-scale losses and jitter frequently degrade performance and user experience. Deploying BIFROST between egress PoPs and the cloud backbone significantly improves reliability and stability.

Real-time video services. Real-time video streaming imposes strict frame deadlines, where transient packet loss or jitter directly manifests as buffering or quality degradation. By providing rapid, transport-layer recovery without requiring application changes, BIFROST sustains smooth delivery even under high-bitrate HD and 4K flows.

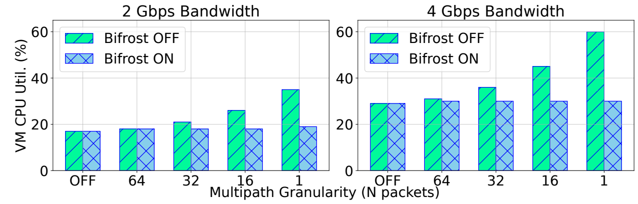

Figure 23: VM CPU util. reduction from BIFROST offload.

7.3 Handling HoL Blocking Issue

Balancing scalability and isolation. Any connection reuse scheme risks introducing HoL blocking, especially when multiple flows are multiplexed over the same logical connection. The aggregation granularity thus presents a trade-off: coarser levels save more state but increase interference risk. Aggregating at the VM-pair level could merge traffic from different containers, causing intra-VM contention, while AVS-pair aggregation would mix traffic across tenants, compromising isolation. We adopt vNIC-pair-level aggregation, which reduces BIFROST connections by over 70% compared to per-5-tuple state. This captures most memory savings while confining HoL blocking to well-defined endpoints like container or tenant interfaces, preserving both scalability and isolation.

Mitigating residual HoL effects. Within a single vNIC, although HoL blocking can theoretically occur when one flow is stalled (*e.g.,* due to loss or congestion), BIFROST mitigates this issue via fast loss recovery, minimizing its impact. In extreme cases where all available paths fail and HoL persists, BIFROST falls back to the original VPC logic, reverting to best-effort UDP delivery to ensure basic connectivity.

7.4 Reorder Tradeoff Across Kernel Versions

Based on our deployment experience, we observe that the necessity of reordering offload heavily depends on the guest kernel version. In recent Linux kernels that support TCP RACK-TLP [24], the transport stack is more tolerant to out-of-order packets. In these environments, we we leave it to the user to decide whether to enable the reordering functionality of BIFROST. When reordering is disabled, guest TCP handles out-of-order arrivals, which reduces memory pressure on the CIPU and allows support for a larger number of concurrent connections. However, under severe reordering, common in fine-grained multipath scenarios, we find that guest-side reordering can consume substantial CPU resources, degrading application performance. To quantify this effect, we conduct an experiment by varying the multipath granularity and measuring the receiver CPU utilization. As shown in Figure 23, finer-grained packet spraying leads to more intense packet reordering, which increases CPU overhead when reordering is handled in the guest kernel. In contrast, enabling BIFROST's reordering reduces CPU consumption by offloading reordering to the CIPU. When BIFROST reordering is enabled, we automatically disable guest-side reordering logic by setting `tcp_recovery=0` and lowering `tcp_max_reordering`, so that all reordering is handled in the CIPU without duplicating effort inside the VM. This tradeoff between VM CPU usage and CIPU memory consumption highlights the need for flexible control, and we provide a per-VNI knob to adapt to different deployment needs.

7.5 Pitfalls and Mitigation of Delayed Release

We face three major issues with sender-side delayed release.

Sender window configuration. Since delayed release pins packets in the VM's buffer until acknowledged, the window must not exceed the VM's buffer capacity, which is bounded by the default ring size of 4096 entries. In practice, we set the initial window to 512, as this value already matches the bandwidth–delay product (BDP) of the longest RTT observed in Alibaba Cloud, providing sufficient pipeline depth without overcommitting VM buffers.

Descriptor starvation under loss. Under heavy loss and retransmission, descriptors may remain unreturned for a long time. This quickly exhausts VM buffers and can trigger head-of-line blocking or even application-level failures. To address this, we configure a timeout: if a packet remains unacknowledged after three consecutive RTO failures ($\approx$28 ms), the CIPU forcibly releases it and updates the used ring. This ensures timely buffer reclamation under persistent stalls, preventing buffer exhaustion and mitigating cascading failures.

Unsafe reuse of TX buffers. Although NAPI-TX is enabled by default and widely used in Alibaba Cloud, we still need to handle corner cases where the VM OS disables NAPI-TX or employs user-space drivers that aggressively recycle buffers. In such cases, delayed release becomes unsafe: the CIPU may retransmit a buffer that has already been overwritten with new data, leading to corrupted packets. To solve this, we implement an adaptive fallback mechanism. Initially, delayed release is disabled and the CIPU caches full packets. Upon the first retransmission, the CIPU compares the current buffer checksum with the cached packet. If they match, indicating no early reuse (*e.g.,* NAPI-TX), delayed release is enabled for subsequent transmissions. Otherwise, the connection remains in full-packet caching mode to ensure correctness.

8 Related Work

Multipath transmission in data center. Multipath transmission has long been explored as a means to mitigate congestion and failures in datacenter networks. Some systems focus on *flow-level* schemes such as PLB [52] and FlowBender [35], which dynamically schedule flows across multiple paths but suffer from coarse granularity and poor responsiveness under elephant flows. To capture finer dynamics, *flowlet-based* mechanisms including LetFlow [71] and HULA [37] split traffic into bursts (flowlets) and distribute them across paths, leveraging transient gaps in packet transmissions to reduce reordering. More recent designs move to *packet-level spraying*, such as SRD [57] , Strack [38], and Conweave [65], where packets are distributed across multiple available paths to provide fast failover and fine-grained balancing, and inevitably lead to more OOO packets. Similar ideas have also been explored in RDMA [21, 38, 62, 65], following the same design direction but with different implementation choices.

Out-of-order transmission. Packet spraying is inherently OOO delivery, which requires reordering before packets can be consumed by the transport stack. Several works [2, 59, 60, 64, 65, 75] explore in-network packet reordering, leveraging programmable switches to align OOO packets. Some other approaches [43, 62, 77] instead rely on reorder buffers at end-host NICs to handle OOO delivery, avoiding reliance on in-network devices. In contrast, some designs [12, 53] eliminate reordering by using Direct Data Placement (DDP), which places packets directly into target memory offsets.

Transport stack offload. Several production systems [38, 57, 62, 69] and research efforts have explored transport stack offload to improve reliability and latency. AWS SRD [57, 58] is a reliable transport protocol offloaded to AWS's custom Nitro cards [17], which uses packet-level spraying to provide low-latency communication in EFA and ENA Express [18, 19]. Google Falcon [62] is a hardware transport for Ethernet datacenters that supports multiple upper layer protocols with delay-based congestion control, multipath load balancing, and hardware retransmissions. Tesla TTPoE [69] is a hardware transport protocol deployed in the Tesla Dojo system [70], designed to replace TCP for large-scale machine learning workloads with low-latency transport over Ethernet. Ultra Ethernet Transport [33] is a hardware transport protocol by the Ultra Ethernet Consortium for scalable, low-latency, and reliable Ethernet communication in AI/ML and HPC networks.

9 Conclusion

In this paper, we present BIFROST, a high-performance multipath RT framework in Alibaba VPC network. BIFROST addresses three long-standing challenges in cloud transport: (i) mitigating reordering overhead under limited SmartNIC memory via in-place guest reordering, (ii) achieving end-to-end reliability coverage via bitmap-based delayed ACK, and (iii) maintaining scalability with efficient reliability state management. Our extensive evaluation shows that BIFROST reduces tail latency by up to 307$\times$ for latency-sensitive services such as Redis. More broadly, our experience indicates that building high-performance multipath RT in clouds is not merely a protocol design problem but a systems-level problem, requiring co-design across virtualization, hardware offload, and resource management. We believe the principles from BIFROST can guide academia and cloud vendors in building high-performance multipath RT for large-scale clouds.

References

[1] Mohammad Al-Fares, Sivasankar Radhakrishnan, Barath Raghavan, Nelson Huang, Amin Vahdat, et al. Hedera: dynamic flow scheduling for data center networks. In *Nsdi*, volume 10, pages 89–92. San Jose, USA, 2010.

[2] Albert Gran Alcoz, Alexander Dietmüller, and Laurent Vanbever. SP-PIFO: Approximating Push-In First-Out behaviors using Strict-Priority queues. In *17th USENIX Symposium on Networked Systems Design and Implementation (NSDI 20)*, pages 59–76, Santa Clara, CA, February 2020. USENIX Association.

[3] Alibaba Cloud. Overview of Flowlog. https://www.alibabacloud.com/help/en/virtual-private-cloud/latest/flow-logs-overview, 2023.

[4] Alibaba Cloud. Traffic Mirroring Overview. https://www.alibabacloud.com/help/en/virtual-private-cloud/latest/traffic-mirroring-overview, 2023.

[5] Alibaba Cloud. Network acl overview. https://www.alibabacloud.com/help/en/vpc/network-acl-overview, 2024. Accessed: 2024-04-05.

[6] Alibaba Cloud. Vpc route table. https://www.alibabacloud.com/help/en/vpc/vpc-route-table/, 2024. Accessed: 2024-06-05.

[7] Alibaba Cloud. Alibaba cloud cloud enterprise network (cen). https://www.alibabacloud.com/en/product/cen, 2025. Accessed: 2025-08-12.

[8] Alibaba Cloud. Api gateway. https://www.alibabacloud.com/en/product/api-gateway?_p_lc=1&spm=a3c0i.179194.6791778070.2.3e5a3a70e4Fnwy, 2025.

[9] Alibaba Cloud. Server load balancer. https://www.alibabacloud.com/en/product/server-load-balancer?_p_lc=1&spm=a3c0i.7911826.2564562790.4.6a323870SZ7vLu, 2025.

[10] Alibaba Cloud. Transit router. https://www.alibabacloud.com/en/product/transit_router?_p_lc=1&spm=a3c0i.7911826.2564562790.1.6a323870SZ7vLu, 2025.

[11] Alibaba Cloud. Virtual private cloud (vpc). https://www.alibabacloud.com/en/product/vpc?_p_lc=1, 2025.

[12] Alibaba Cloud Documentation Center. Elastic compute service: erdma. Online; last updated August 1, 2025, 2025. Alibaba Cloud Help — User Guide, Network section: eRDMA.

[13] Mohammad Alizadeh, Tom Edsall, Sarang Dharmapurikar, Ramanan Vaidyanathan, Kevin Chu, Andy Fingerhut, Vinh The Lam, Francis Matus, Rong Pan, Navindra Yadav, et al. Conga: Distributed congestion-aware load balancing for datacenters. In *Proceedings of the 2014 ACM conference on SIGCOMM*, pages 503–514, 2014.

[14] Amazon Web Services. Logging IP Traffic Using VPC Flow Logs. https://docs.aws.amazon.com/vpc/latest/userguide/flow-logs.html, 2021.

[15] Amazon Web Services. Amazon Virtual Private Cloud Traffic Mirroring. https://docs.aws.amazon.com/vpc/latest/mirroring/what-is-traffic-mirroring.html, 2022.

[16] Amazon Web Services. Amazon vpc documentation. https://docs.aws.amazon.com/vpc/, 2024.

[17] Amazon Web Services. Aws nitro system. https://aws.amazon.com/ec2/nitro/, 2025. Accessed: 2025-08-26.

[18] Amazon Web Services. Elastic fabric adapter (efa). https://docs.aws.amazon.com/AWSEC2/latest/UserGuide/efa.html, 2025. Accessed: 2025-08-26.

[19] Amazon Web Services. Ena express. https://docs.aws.amazon.com/AWSEC2/latest/UserGuide/ena-express.html, 2025. Accessed: 2025-08-26.

[20] Theophilus Benson, Ashok Anand, Aditya Akella, and Ming Zhang. Microte: Fine grained traffic engineering for data centers. In *Proceedings of the seventh conference on emerging networking experiments and technologies*, pages 1–12, 2011.

[21] Tommaso Bonato, Abdul Kabbani, Ahmad Ghalayini, Michael Papamichael, Mohammad Dohadwala, Lukas Gianinazzi, Mikhail Khalilov, Elias Achermann, Daniele De Sensi, and Torsten Hoefler. Arcane: Adaptive routing with caching and aware network exploration, 2025.

[22] Olivier Bonaventure, Christoph Paasch, and Gregory Detal. Use cases and operational experience with multipath tcp. Technical report, 2017.

[23] Lucas Chaufournier, Ahmed Ali-Eldin, Prateek Sharma, Prashant Shenoy, and Don Towsley. Performance evaluation of multi-path tcp for data center and cloud workloads. In *Proceedings of the 2019 ACM/SPEC International Conference on Performance Engineering*, pages 13–24, 2019.

[24] Yuchung Cheng, Neal Cardwell, Nandita Dukkipati, and Priyaranjan Jha. The RACK-TLP Loss Detection Algorithm for TCP. RFC 8985, February 2021.

[25] Alibaba Cloud. A detailed explanation about alibaba cloud cipu. https://www.alibabacloud.com/blog/599183, 2023.

[26] Andrew R Curtis, Wonho Kim, and Praveen Yalagandula. Mahout: Low-overhead datacenter traffic management using end-host-based elephant detection. In *2011 Proceedings IEEE INFOCOM*, pages 1629–1637. IEEE, 2011.

[27] DPDK Project. Data plane development kit (dpdk), 2024. Accessed: 2024-06-10.

[28] Zihao Fan, Enge Song, Bo Jiang, Yang Song, Yuke Hong, Bowen Yang, Yilong Lv, Yinian Zhou, Junnan Cai, Chao Wang, Yi Wang, Yehao Feng, Dian Fan, Ye Yang, Shize Zhang, Xiaoqing Sun, Jianyuan Lu, Xing Li, Jun Liang, Biao Lyu, Zhigang Zong, and Shunmin Zhu. Understanding the long tail latency of tcp in large-scale cloud networks. In *Proceedings of the 9th Asia-Pacific Workshop on Networking*, APNET '25, page 106–113, New York, NY, USA, 2025. Association for Computing Machinery.

[29] Alan Ford, Costin Raiciu, Mark Handley, and Olivier Bonaventure. Tcp extensions for multipath operation with multiple addresses. Technical report, 2013.

[30] Yilong Geng, Vimalkumar Jeyakumar, Abdul Kabbani, and Mohammad Alizadeh. Juggler: a practical reordering resilient network stack for datacenters. In *Proceedings of the Eleventh European Conference on Computer Systems*, pages 1–16, 2016.

[31] Soudeh Ghorbani, Zibin Yang, P Brighten Godfrey, Yashar Ganjali, and Amin Firoozshahian. Drill: Micro load balancing for low-latency data center networks. In *Proceedings of the Conference of the ACM Special Interest Group on Data Communication*, pages 225–238, 2017.

[32] Google Cloud. Virtual private cloud (vpc). https://cloud.google.com/vpc, 2025.

[33] Torsten Hoefler, Karen Schramm, Eric Spada, Keith Underwood, Cedell Alexander, Bob Alverson, Paul Bottorff, Adrian Caulfield, Mark Handley, Cathy Huang, Costin Raiciu, Abdul Kabbani, Eugene Opsasnick, Rong Pan, Adee Ran, and Rip Sohan. Ultra ethernet's design principles and architectural innovations, 2025.

[34] Intel Corporation. Infrastructure processing unit (ipu), 2024. Accessed: 2024-06-10.

[35] Abdul Kabbani, Balajee Vamanan, Jahangir Hasan, and Fabien Duchene. Flowbender: Flow-level adaptive routing for improved latency and throughput in datacenter networks. In *Proceedings of the 10th ACM International on Conference on emerging Networking Experiments and Technologies*, pages 149–160, 2014.

[36] Naga Katta, Aditi Ghag, Mukesh Hira, Isaac Keslassy, Aran Bergman, Changhoon Kim, and Jennifer Rexford. Clove: Congestion-aware load balancing at the virtual edge. In *Proceedings of the 13th International Conference on emerging Networking EXperiments and Technologies*, pages 323–335, 2017.

[37] Naga Katta, Mukesh Hira, Changhoon Kim, Anirudh Sivaraman, and Jennifer Rexford. Hula: Scalable load balancing using programmable data planes. In *Proceedings of the Symposium on SDN Research*, pages 1–12, 2016.

[38] Yanfang Le, Rong Pan, Peter Newman, Jeremias Blendin, Abdul Kabbani, Vipin Jain, Raghava Sivaramu, and Francis Matus. Strack: A reliable multipath transport for ai/ml clusters, 2024.

[39] Xing Li, Xiaochong Jiang, Ye Yang, Lilong Chen, Yi Wang, Chao Wang, Chao Xu, Yilong Lv, Bowen Yang, Taotao Wu, et al. Triton: A flexible hardware offloading architecture for accelerating apsara vswitch in alibaba cloud. In *Proceedings of the ACM SIGCOMM 2024 Conference*, pages 750–763, 2024.

[40] Xing Li, Enge Song, Bowen Yang, Tian Pan, Ye Yang, Qiang Fu, Yang Song, Yilong Lv, Zikang Chen, Jianyuan Lu, Shize Zhang, Xiaoqing Sun, Rong Wen, Xionglie Wei, Biao Lyu, Zhigang Zong, Qinming He, and Shunmin Zhu. Nezha: Smartnic-based virtual switch load sharing. In *Proceedings of the ACM SIGCOMM 2025 Conference*, ACM SIGCOMM '25, New York, NY, USA, 2025. Association for Computing Machinery.

[41] Jingling Liu, Jiawei Huang, Wenjun Lv, and Jianxin Wang. Aps: Adaptive packet spraying to isolate mixflows in data center network. *IEEE Transactions on Cloud Computing*, 10(2):1038–1051, 2020.

[42] Jianyuan Lu, Tian Pan, Shan He, Mao Miao, Guangzhe Zhou, Yining Qi, Shize Zhang, Enge Song, Xiaoqing Sun, Huaiyi Zhao, et al. Cloudsentry: Two-stage heavy

hitter detection for cloud-scale gateway overload protection. *IEEE Transactions on Parallel and Distributed Systems*, 35(4):616–633, 2023.

[43] Jianyuan Lu, Shunmin Zhu, Jun Liang, Yuxiang Lin, Tian Pan, Yisong Qiao, Yang Song, Wenqiang Su, Yixin Xie, Yanqiang Li, Enge Song, Shize Zhang, Xiaoqing Sun, Rong Wen, Xionglie Wei, Biao Lyu, and Xing Li. Albatross: A containerized cloud gateway platform with fpga-accelerated packet-level load balancing. In *Proceedings of the ACM SIGCOMM 2025 Conference*, ACM SIGCOMM '25, New York, NY, USA, 2025. Association for Computing Machinery.

[44] Jie Lu, Jiaqi Gao, Fei Feng, Zhiqiang He, Menglei Zheng, Kun Liu, Jun He, Binbin Liao, Suwei Xu, Ke Sun, Yongjia Mo, Qinghua Peng, Jilie Luo, Qingxu Li, Gang Lu, Zishu Wang, Jianbo Dong, Kunling He, Sheng Cheng, Jiamin Cao, Hairong Jiao, Pengcheng Zhang, Shu Ma, Lingjun Zhu, Chao Shi, Yangming Zhang, Yiquan Chen, Wei Wang, Shuhong Zhu, Xingru Li, Qiang Wang, Jiang Liu, Chao Wang, Wei Lin, Ennan Zhai, Jiesheng Wu, Qiang Liu, Binzhang Fu, and Dennis Cai. Alibaba stellar: A new generation rdma network for cloud ai. In *Proceedings of the ACM SIGCOMM 2025 Conference*, SIGCOMM '25, page 453–466, New York, NY, USA, 2025. Association for Computing Machinery.

[45] Microsoft Azure. Azure virtual network – virtual private cloud. https://azure.microsoft.com/en-us/products/virtual-network, 2025.

[46] MongoDB Inc. Mongodb, 2024. [Online]. Available: https://www.mongodb.com/.

[47] NVIDIA. Nvidia bluefield networking platform. https://www.nvidia.com/en-us/networking/products/data-processing-unit/, 2025. Accessed: 2025.

[48] NVIDIA Corporation. DPA Subsystem — NVIDIA DOCA SDK. https://docs.nvidia.com/doca/sdk/DPA%2BSubsystem/index.html, 2025. Accessed: 27 August 2025.

[49] Oracle Corporation. Mysql. https://www.mysql.com, 2024.

[50] Tian Pan, Nianbing Yu, Chenhao Jia, Jianwen Pi, Liang Xu, Yisong Qiao, Zhiguo Li, Kun Liu, Jie Lu, Jianyuan Lu, et al. Sailfish: Accelerating cloud-scale multi-tenant multi-service gateways with programmable switches. In *Proceedings of the 2021 ACM SIGCOMM 2021 Conference*, pages 194–206, 2021.

[51] Jonathan Perry, Amy Ousterhout, Hari Balakrishnan, Devavrat Shah, and Hans Fugal. Fastpass: A centralized" zero-queue" datacenter network. In *Proceedings of the 2014 ACM conference on SIGCOMM*, pages 307–318, 2014.

[52] Mubashir Adnan Qureshi, Yuchung Cheng, Qianwen Yin, Qiaobin Fu, Gautam Kumar, Masoud Moshref, Junhua Yan, Van Jacobson, David Wetherall, and Abdul Kabbani. Plb: congestion signals are simple and effective for network load balancing. In *Proceedings of the ACM SIGCOMM 2022 Conference*, pages 207–218, 2022.

[53] Mohammad J. Rashti and Ahmad Afsahi. 10-gigabit iwarp ethernet: Comparative performance analysis with infiniband and myrinet-10g. In *2007 IEEE International Parallel and Distributed Processing Symposium*, pages 1–8, 2007.

[54] Redis Ltd. Redis, 2024. [Online]. Available: https://redis.io/.

[55] Rusty Russell. virtio: towards a de-facto standard for virtual i/o devices. *SIGOPS Oper. Syst. Rev.*, 42(5):95–103, July 2008.

[56] Siddhartha Sen, David Shue, Sunghwan Ihm, and Michael J Freedman. Scalable, optimal flow routing in datacenters via local link balancing. In *Proceedings of the ninth ACM conference on Emerging networking experiments and technologies*, pages 151–162, 2013.

[57] Leah Shalev, Hani Ayoub, Nafea Bshara, Yuval Fatael, Ori Golan, Omer Ilany, Anna Levin, Zorik Machulsky, Kevin Milczewski, Marc Olson, et al. The tail at aws scale. *IEEE Micro*, 2024.

[58] Leah Shalev, Hani Ayoub, Nafea Bshara, and Erez Sabbag. A cloud-optimized transport protocol for elastic and scalable hpc. *IEEE micro*, 40(6):67–73, 2020.

[59] Naveen Kr. Sharma, Ming Liu, Kishore Atreya, and Arvind Krishnamurthy. Approximating fair queueing on reconfigurable switches. In *15th USENIX Symposium on Networked Systems Design and Implementation (NSDI 18)*, pages 1–16, Renton, WA, April 2018. USENIX Association.

[60] Naveen Kr. Sharma, Chenxingyu Zhao, Ming Liu, Pravein G Kannan, Changhoon Kim, Arvind Krishnamurthy, and Anirudh Sivaraman. Programmable calendar queues for high-speed packet scheduling. In *17th USENIX Symposium on Networked Systems Design and Implementation (NSDI 20)*, pages 685–699, Santa Clara, CA, February 2020. USENIX Association.

[61] Dian Shen, Bin Yang, Junxue Zhang, Fang Dong, and John CS Lui. emptcp: A framework to fully extend multipath tcp. *IEEE/ACM Transactions on Networking*, 2024.

[62] Arjun Singhvi, Nandita Dukkipati, Prashant Chandra, Hassan M. G. Wassel, Naveen Kr. Sharma, Anthony Rebello, Henry Schuh, Praveen Kumar, Behnam Montazeri, Neelesh Bansod, Sarin Thomas, Inho Cho, Hyojeong Lee Seibert, Baijun Wu, Rui Yang, Yuliang Li, Kai Huang, Qianwen Yin, Abhishek Agarwal, Srinivas Vaduvatha, Weihuang Wang, Masoud Moshref, Tao Ji, David Wetherall, and Amin Vahdat. Falcon: A reliable, low latency hardware transport. In *Proceedings of the ACM SIGCOMM 2025 Conference*, SIGCOMM '25, page 248–263, New York, NY, USA, 2025. Association for Computing Machinery.

[63] Shan Sinha, Srikanth Kandula, and Dina Katabi. Harnessing tcp's burstiness with flowlet switching. In *Proc. 3rd ACM Workshop on Hot Topics in Networks (Hotnets-III)*. Citeseer, 2004.

[64] Anirudh Sivaraman, Suvinay Subramanian, Mohammad Alizadeh, Sharad Chole, Shang-Tse Chuang, Anurag Agrawal, Hari Balakrishnan, Tom Edsall, Sachin Katti, and Nick McKeown. Programmable packet scheduling at line rate. In *Proceedings of the 2016 ACM SIGCOMM Conference*, SIGCOMM '16, page 44–57, New York, NY, USA, 2016. Association for Computing Machinery.

[65] Cha Hwan Song, Xin Zhe Khooi, Raj Joshi, Inho Choi, Jialin Li, and Mun Choon Chan. Network load balancing with in-network reordering support for rdma. In *Proceedings of the ACM SIGCOMM 2023 Conference*, ACM SIGCOMM '23, page 816–831, New York, NY, USA, 2023. Association for Computing Machinery.

[66] Enge Song, Nianbing Yu, Tian Pan, Qiang Fu, Liang Xu, Xionglie Wei, Yisong Qiao, Jianyuan Lu, Yijian Dong, Mingxu Xie, et al. Mimic: Smartnic-aided flow backpressure for cpu overloading protection in multi-tenant clouds. In *2022 IEEE 30th International Conference on Network Protocols (ICNP)*, pages 1–11. IEEE, 2022.

[67] Xiaoqing Sun, Xionglie Wei, Xing Li, Ju Zhang, Bowen Yang, Yi Wang, Ye Yang, Yu Qi, Le Yu, Chenhao Jia, Zhanlong Zhang, Xinyu Chen, Jianyuan Lu, Shize Zhang, Enge Song, Yang Song, Tian Pan, Rong Wen, Biao Lyu, Yang Xu, and Shunmin Zhu. Zooroute: Enhancing cloud-scale network reliability via overlay proactive rerouting. In *Proceedings of the ACM SIGCOMM 2025 Conference*, SIGCOMM '25, page 1251–1253, New York, NY, USA, 2025. Association for Computing Machinery.

[68] Igor Sysoev. Nginx: An http and reverse proxy server. https://nginx.org, 2004. Accessed: 2025-02-28.

[69] Tesla. TTPoE: Tesla Transport Protocol over Ethernet. https://github.com/teslamotors/ttpoe, 2024. GitHub repository.

[70] Tesla, Inc. Tesla ai. https://www.tesla.com/en_gb/AI, 2025. Accessed: 2025-08-26.

[71] Erico Vanini, Rong Pan, Mohammad Alizadeh, Parvin Taheri, and Tom Edsall. Let it flow: Resilient asymmetric load balancing with flowlet switching. In *14th USENIX Symposium on Networked Systems Design and Implementation (NSDI 17)*, pages 407–420, 2017.

[72] Peng Wang, Hong Xu, Zhixiong Niu, Dongsu Han, and Yongqiang Xiong. Expeditus: Congestion-aware load balancing in clos data center networks. In *Proceedings of the Seventh ACM Symposium on Cloud Computing*, pages 442–455, 2016.

[73] Chengkun Wei, Xing Li, Ye Yang, Xiaochong Jiang, Tianyu Xu, Bowen Yang, Taotao Wu, Chao Xu, Yilong Lv, Haifeng Gao, et al. Achelous: Enabling programmability, elasticity, and reliability in hyperscale cloud networks. In *Proceedings of the ACM SIGCOMM 2023 Conference*, pages 769–782, 2023.

[74] Xin Yin, Enge Song, Ye Yang, Yi Wang, Bowen Yang, Jianyuan Lu, Xing Li, Biao Lyu, Rong Wen, Shibo He, Yuanchao Shu, and Shunmin Zhu. vswitchlb: Stratified load balancing for vswitch efficiency in data centers. In *Proceedings of the 8th Asia-Pacific Workshop on Networking*, APNet '24, page 95–101, New York, NY, USA, 2024. Association for Computing Machinery.

[75] Zhuolong Yu, Chuheng Hu, Jingfeng Wu, Xiao Sun, Vladimir Braverman, Mosharaf Chowdhury, Zhenhua Liu, and Xin Jin. Programmable packet scheduling with a single queue. In *Proceedings of the 2021 ACM SIGCOMM 2021 Conference*, SIGCOMM '21, page 179–193, New York, NY, USA, 2021. Association for Computing Machinery.

[76] David Zats, Tathagata Das, Prashanth Mohan, Dhruba Borthakur, and Randy Katz. Detail: Reducing the flow completion time tail in datacenter networks. In *Proceedings of the ACM SIGCOMM 2012 conference on Applications, technologies, architectures, and protocols for computer communication*, pages 139–150, 2012.

[77] David Zats, Tathagata Das, Prashanth Mohan, Dhruba Borthakur, and Randy Katz. Detail: reducing the flow completion time tail in datacenter networks. *SIGCOMM Comput. Commun. Rev.*, 42(4):139–150, August 2012.

[78] Hong Zhang, Junxue Zhang, Wei Bai, Kai Chen, and Mosharaf Chowdhury. Resilient datacenter load balancing in the wild. In *Proceedings of the Conference of the ACM Special Interest Group on Data Communication*, pages 253–266, 2017.

[79] Tao Zhang, Ran Huang, Yuanzhen Hu, Yangfan Li, Shaojun Zou, Qianqiang Zhang, Xin Liu, and Chang Ruan. Load balancing with deadline-driven parallel data transmission in data center networks. *IEEE Internet of Things Journal*, 10(2):1171–1191, 2022.

[80] Zhilong Zheng, Yunfei Ma, Yanmei Liu, Furong Yang, Zhenyu Li, Yuanbo Zhang, Jiuhai Zhang, Wei Shi, Wentao Chen, Ding Li, et al. Xlink: Qoe-driven multi-path quic transport in large-scale video services. In *Proceedings of the 2021 ACM SIGCOMM 2021 Conference*, pages 418–432, 2021.

Appendices

A VPC and VM Growth Trends

To provide context on the scale of our production environment, Figure A1 shows the growth of VPCs and VMs in Alibaba Cloud over the past five years. As the left panel illustrates, the number of VPCs has more than doubled from 3 trillion in 2020 to nearly 8 trillion in 2024. Meanwhile, the right panel shows that the number of VMs per VPC has also grown rapidly, reaching over 170 million by 2024. These trends underscore the role of VPC as the foundation of cloud networking, supporting massive tenant isolation and elastic resource management at scale.

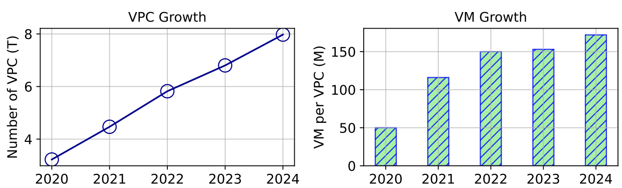

Figure A1: Growth of VPCs (left) and VMs per VPC (right) in Alibaba Cloud.

B Production Case Studies

In this section, we presents a series of representative operational incidents encountered during Alibaba Cloud's production operations, illustrating key failure scenarios, their root causes, and the resulting impact on customer services.

B.1 Host-Side Cases

Bitter Case I: *Jun 2, 2022 — Monitoring detected a single-sided NIC fault on a customer server, causing intermittent timeouts in business container access to the database for approximately 176 minutes.*

Bitter Case II: *Nov 22, 2021 — Single-side NIC flapping on customer server caused intermittent network connectivity and business disruption, lasting approximately 141 minutes.*

B.2 Network-Side Cases

Bitter Case III: *May 23, 2022 — Spine switch malfunction caused network packet loss and elevated error rates in business services, resulting in approximately 184 minutes of service disruption.*

Bitter Case IV: *Mar 4, 2022 — An integrated access switch anomaly caused intermittent packet drops, degrading latency-sensitive advertising services for over 60 minutes, despite the core-side fault lasting only ∼20 minutes.*

B.3 Middlebox Cases

Bitter Case V: *Aug 16, 2024 — A sudden traffic surge overwhelmed the packet transformation of network load balancer, causing continuous packet losses for 14 minutes.*

C Protocol Specification

Data Packet Header. The BIFROST data packet header (Figure C2) encodes control and reliability information in a compact format. The header starts with the `Pkt Type` field (8 bits), indicating whether the packet is used for data transmission, acknowledgment, or connection management. It is followed by a `Version` field (4 bits) for protocol compatibility and a `CC Type` field (4 bits) specifying the active congestion control algorithm. A set of 1-bit control flags refine transport semantics: `se` marks special packet types such as keepalive, `ack` indicates whether acknowledgment is required, `dir` specifies the packet direction, `ece` enables explicit congestion notification, and `ret` identifies retransmitted packets. A 3-bit `Path ID` field identifies designated paths within a multipath connection and enables packet-level steering. An 8-bit `Reserved` field is preserved for future extensions. Beyond these control fields, the header carries a `Packet Sequence Number` (32 bits) to support reliable delivery, a `Destination CID` (32 bits) to identify the receiving connection, and a `Timestamp Value` (32 bits) for RTT estimation and congestion control.

Bits 0-7	8-11	12-15	16	17	18	19	20	21-23	24-31
Pkt Type	Version	CC Type	se	ack	dir	ece	ret	Path ID	Reserved
Packet Sequence Number (PSN)									
Destination Connection ID (CID)									
Timestamp Value									

Figure C2: BIFROST data packet header.

Connection Establishment Packet Header. The BIFROST connection establishment packet header (Figure C3) largely follows the same structure as the data packet header, beginning with the `Pkt Type` (8 bits), `Version` (4 bits), and `CC Type` (4 bits) fields, followed by a `Thread ID` (8 bits) to facilitate core affinity and an 8-bit Reserved field for future use. In addition to the `Destination CID` (32 bits) already carried by data packets, the header also includes a `Local CID` (32 bits). This extra identifier allows both endpoints to exchange and bind their CIDs during the handshake, ensuring consistent connection mapping for subsequent reliable transmission.

Bits 0-7	8-11	12-15	16-23	24-31
Pkt Type	Version	CC Type	Thread ID	Reserved
Local CID				
Destination CID				

Figure C3: BIFROST connection establishment packet header.

ACK Packet Header. The BIFROST ACK packet header consolidates both basic control fields and bitmap-based acknowledgment information. The header begins with `Pkt Type` (8 bits), indicating the packet type. The `Path ID` (3 bits) also identifies designated paths of multipath transmission. The `Packet Sequence Number` (32 bits) and `Destination CID` (32 bits) carry the same semantics as in data packets. To support congestion control and RTT estimation, the header further embeds three timestamps: `Timestamp Value` (32 bits) generated at packet transmission, `Timestamp Echo` (32 bits) carrying the sender's timestamp for RTT calculation, and `Timestamp NIC RX` (32 bits) recording the NIC reception time. Additional lightweight fields include `ACK Type` (3 bits), `ACK Value` (5 bits) for extended acknowledgment semantics, `Hop Count` (4 bits) to measure the number of forwarding hops, and the `se` flag (1 bit) to mark special packet types such as keepalive.

On top of these, the header incorporates a bitmap-based acknowledgment scheme. Specifically, `Num_ACK` (11 bits) records the number of acknowledged packets, `Num_ECE` (11 bits) counts congestion marks, and `PSN_bitmap_len` (4 bits) specifies the bitmap length. The acknowledgment range is anchored by `PSN_base` (32 bits), followed by up to eight `PSN_bitmap[·]` (32 bits each) fields, which encode the reception state of consecutive packets. This compact structure enables a single ACK packet to cumulatively acknowledge up to 256 packets, providing fast and precise feedback for loss recovery and congestion control.

Bits 0-7	8-11	12-15	16	17-19	20-23	24-28	29-31
Pkt Type	Version	CC Type	se	Path ID	Hop Count	ACK Value	ACK Type
Packet Sequence Number (PSN)							
Destination CID							
Timestamp Value							
Timestamp Echo							
Timestamp NIC RX							
Num_ACK		Num_ece		PSN_bitmap_len		Reserved	
PSN_base							
PSN_bitmap[0]							
PSN_bitmap[1]							
PSN_bitmap[2]							
PSN_bitmap[3]							
PSN_bitmap[4]							
PSN_bitmap[5]							
PSN_bitmap[6]							
PSN_bitmap[7]							

Figure C4: BIFROST ACK header.

D Detailed Pipeline of Delayed Release

The most straightforward approach to achieving reliable packet transmission is to let the CIPU cache all unacknowledged packets in its local memory, as illustrated in Figure D5 (left). Specifically, when the CIPU sends a packet, it retains the full payload in memory (②) until the ACK is received from the receiver, after which the buffer is finally released (⑤). Under high connection concurrency, this quickly consumes memory and is particularly challenging given the CIPU's limited capacity. To address this, BIFROST introduces a sender-

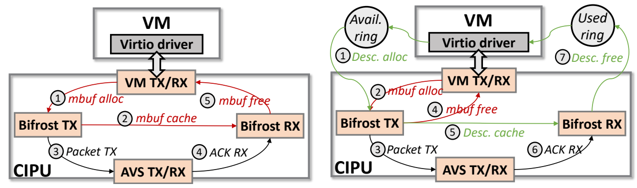

Figure D5: Sender-side delayed release mechanism: (Left) without delayed release and (Right) with delayed release.

side delayed release mechanism that shifts the packet buffering responsibility from the CIPU to the tenant VM, as shown in Figure D5 (right). When transmitting a packet, the CIPU first fetches the *descriptors* from the avail ring (①). Instead of caching the full packet in its local memory, the CIPU only stores the lightweight descriptors for potential retransmission (④⑤), while the actual packet remains pinned in the VM's memory. Once an ACK is received (⑥), the CIPU writes the *descriptors* into the *used ring* (⑦), allowing the VM to reclaim the buffer. Since *descriptors* are much smaller than full packets, this design greatly reduces CIPU memory consumption and improves scalability. This mechanism incurs no additional memory overhead on the VM, as its protocol stack (*e.g.,* TCP) already retains the full packet until the corresponding ACK arrives. BIFROST leverages this fact to eliminate redundant packet buffering on the CIPU.

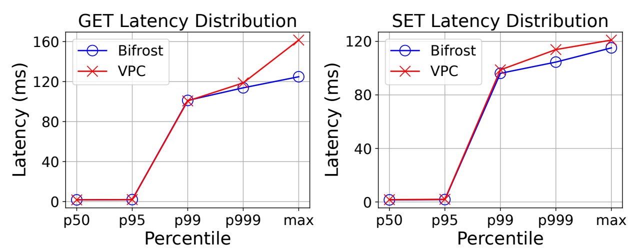

Figure D6: Redis short connection performance.

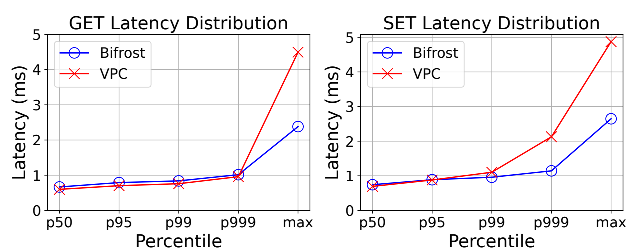

Figure D7: Redis persistent connection performance.

E Supplementary Experiments

E.1 Redis

Redis under stable conditions. We further evaluate Redis in the short-connection mode without injecting artificial loss, using the same setup of two VMs placed on different physical servers. Figure D6 reports the latency distribution for both *get* and *set* operations. Compared to the vanilla VPC,

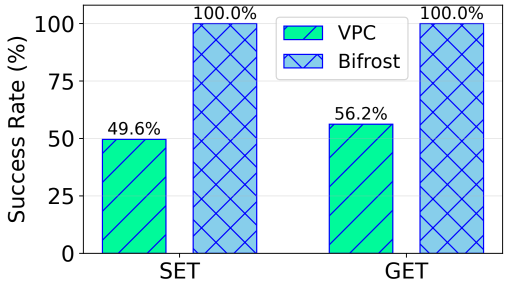

Figure E8: Redis request success rate.

BIFROST incurs negligible overhead in average latency and reduces tail latency at high percentiles (P999 and Max), showing that its mechanisms remain lightweight under relatively stable network conditions. Figure D7 also reports the latency distribution for both *get* and *set* operations of persistent connections, which exhibit the same trend: BIFROST incurs only minimal overhead at lower percentiles while further reducing tail latency at high percentiles.

Request success rate. We further evaluate request success rate when inducing a physical NIC port failure. The experiment uses two VMs on different physical servers, where the client issues *get* and *set* requests to the server to test request success rate. As shown in Figure E8, under the vanilla VPC the success rate drops to 49.6% for *set* and 56.2% for *get*, as requests are disrupted by the failure. In contrast, BIFROST masks the port failure by rerouting traffic across healthy paths, sustaining a 100% success rate for both operations.